DEVELOPMENT OF TWO-STROKE SPARK IGNITION ENGINE WITH MANIFOLD ELECTRONIC CNG INJECTION

S. Kumarappa* G. P. Prabhukumar**

ABSTRACT

In this work, a two-stroke spark ignition engine with manifold electronic gaseous fuel injection system was developed for better fuel economy and reduced emissions. The fuel and time maps were generated for various operating conditions of the engine using an electronic system that is designed to access the data using interfaces. For the mapping, the visualization tool used is a three-dimensional plot. From this mapping, the fuel injection time and delivery quantity were estimated for the required running conditions of the engine. The Experiments were carried out at different speeds with a compression ratio of 12:1. The performance and emission characteristics of the engine with CNG as fuel in carbureted mode and newly developed CNG injection system are described. Investigation was also carried out in the manifold injection mode using CNG as fuel to determine the potential for improving the thermal efficiency of an engine to take advantage of the high octane number of natural gas by varying the compression ratio from 6.7 to 12.

Keywords: Two-stroke spark ignition engine, Manifold injection, CNG, Microcontroller

1. INTRODUCTION

In developed and developing countries considerable emphasis is being laid on the minimization of pollutants from I.C. engines. Two-stroke cycle engine produces considerable amount of pollutants when gasoline is used as a fuel due to short-circuiting. These pollutants, which include unburnt hydrocarbons and carbon monoxide, are harmful to human life. There is a strong need to develop technologies so that the pollution from two stroke engines is minimized. Many techniques like gas carburetor, electronic fuel injection, catalytic converters, lean burn engine concepts [Douglass et al, 1982] and use of alternative fuels are available.

In the recent years increasing prices of petrol, dwindling of fuel reserves, uncertainty in their supply and increasing rates of air pollution have spurred the search for alternative fuels. Alternative fuels like methanol, methanol gasoline blends, ethanol, ethanol gasoline blends, LPG and CNG have been tried. Among all these alternative fuels, CNG seems to be more attractive from the environmental point of view [Richard et al, 1997].

The objectives of present study are:

- To compare the performance of a carbureted and injected engine at different speeds. [RTF bookmark start: OLE_LINK1]
- Performance tests at different compression ratios in the injection mode.

In a lean burn engine, air fuel ratio is extremely critical. Operation near the lean mixture limit is necessary to obtain the lowest possible emission and the best fuel economy. However near the lean limit, a slight error in air-fuel ratio can drive the engine to misfire. This condition causes drastic increase in hydrocarbon emission; engine roughness and

* Bapuji Institute of Engineering and Technology, Davangere, Karnataka, India.
** University BDT College of Engineering, Davangere, Karnataka, India

poor throttle response [Giichi Yamagishi et al, 1972; Edward, 1978 and Pipho et al, 1983]. A reliable electronic gaseous fuel injection system was designed and built in order to control the engine and also for the evaluation of control strategies. The electronic control unit is used to estimate the pulse width of the signal that would actuate the fuel injector and the start of fuel injection. The experiments were carried out on the engine using state of-art instrumentation.

1.1 Fuel Induction Techniques

The performance characteristics of an engine and the concentration level of the exhaust emissions depend, to a large extent, on the combustion pattern. It directly depends on fuel supply system, which provides an appropriate mixture of fuel and air to the engine at the appropriate point in the cycle. The fuel air mixture must be in right proportion as per the condition of the speed and load on the engine. The overall engine behavior depends upon the fuel induction mechanism. Introduction of a CNG kit to the existing gasoline engine hardware does not involve any substantial modifications except inducting the mixture into the intake manifold. However, in spite of the excellent characteristics and various advantages of CNG as a fuel in vehicles, it has certain problems, when used in vehicles, like backfiring during suction, knocking at higher compression ratio with advanced spark timing. These problems are due to inappropriate technology used for the formation of the mixture.

In consideration of the inherent constraints in the design of carburetor, the engine manufacturers and automobile industries now are switching over to fuel injection system [David Gimbres et al, 1999 and Kichiro kato et al, 1999]. The mode of fuel injection from an injector plays a critical role in determining the performance characteristics of an engine. The lean burn for the engine operation can be easily achieved with this technique. Keeping in view the requirement of the CNG fuel, an electronic gaseous fuel injection system was designed and developed in the present experimental work.

1.2 Electronic CNG Injection System

The modern internal combustion engine has to meet the extreme requirements of high power to weight ratio, low exhaust emissions, easy maintenance, and high thermal efficiency. This has been made possible through the extensive use of electronic controls. Electronic control of the injection system allows us to select the correct air- fuel ratio for different operating conditions.

Electronic fuel injection is more efficient than carburetors because it is able to compensate for a variety of operating conditions. This compensating ability allows the system to deliver the optimum fuel mixture needed, resulting in good throttle response and fuel economy.

The most common inputs required are engine speed; throttle position, crank position, and injection duration. The microcontroller receives the signals from the sensors and determines the exact quantity of fuel to be injected per cycle for the particular load and speed conditions of the engine. When the crank rotates, the crank position sensor detects the position of the crankshaft and a signal is generated to interrupt the microcontroller. The microcontroller calculates the injection duration based on the throttle position and speed of previous cycle. The microcontroller generates a pulse to the injector interface unit. The injector interface unit delivers the appropriate voltage and current to the injector, and thus exact metered quantity of fuel is injected. On completion of the injection, the microcontroller once again reads the throttle position, engine speed and calculates the injection duration for the next cycle and waits for the next crank position sensor signal. On line control of the injection duration is also provided through another port for optimization of the engine performance.

2. PERFORMANCE TEST OF MANIFOLD INJECTION SYSTEM

2.1 Modifications in the Intake Manifold

The injector was positioned such that it assists the best fuel mixing. In order to position the injector at the manifold a special adaptor was designed so as to house the injector as shown in Figure 1. In the experimental engine the crankshaft directly controls the opening of the intake port. The injection is timed such that it starts after the crankshaft opens the intake port and the injection stop well before the crankshaft closes the intake port. The throttle body is fixed to the other end of the intake manifold to throttle the air supplied to engine. The throttle position sensor was fixed to the throttle body to sense the throttle opening. The speed sensor, and crankshaft position sensor were fixed to the engine.

2.2 Testing of the Manifold Injection System

The manifold injection system was tested at different speeds of 2500, 3000,3500 and 4000 rpm. The performance was optimized for minimum HC and CO emissions. Initially the microcontroller calculates the injection duration based on the fuel map obtained from the carbureted engine performance at a particular throttle opening and engine speed. This injection duration is varied manually with the help of external switches such that the HC and CO emissions are minimized, without loss of brake power at every load point. The optimized manifold injection(MI) engine performance is compared with the carbureted engine performance.

Investigations were also carried out in the manifold injection mode using CNG as fuel to determine the potential for improving the thermal efficiency of the engine to take advantage of the high octane number of natural gas by varying the compression ratio from 6.7 to 12.

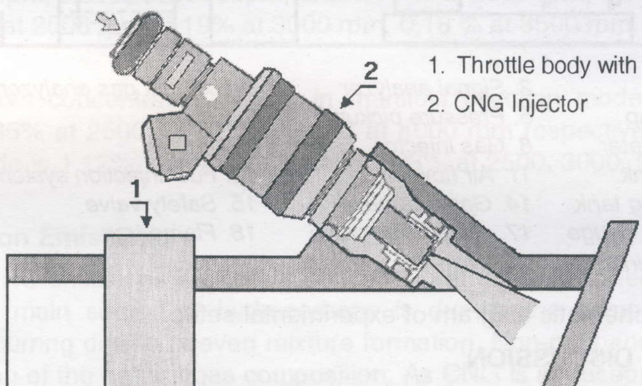

Figure. 1 Modified manifold injector holder

3. EXPERIMENTAL TEST SETUP

A 98 cc, two-stroke spark ignition engine was used in this study. Figure 2 shows the schematic diagram of experimental setup and the engine instrumentation. The fuel system consists of high-pressure storage cylinders with a filling pressure of about 22 MPa, a regulator to reduce the line pressure to 200 kPa and a high-pressure line for connecting the cylinder to the regulator. An injection system controller was used to control the pulse width of the injector. The engine was connected to brake dynamometer for loading purposes. Fuel consumption was measured using weighing machine. Air consumption was measured by an air flow meter.

A pressure transducer in conjunction with a charge amplifier was used to measure the cylinder pressure. The transducer was mounted in the cylinder head. Signals of crankshaft angle were derived from a shaft encoder rigidly attached to the engine crankshaft. The top dead center (TDC) signal of the encoder was checked with the engine TDC, under dynamic conditions. The encoder provides the necessary signals for the data acquisition system to collect cylinder pressure at every degree during engine cycle. The exhaust emissions of HC and CO are measured with an exhaust gas analyzer. The performance testing of the engine is carried out at 2500, 3000, 3500, and 4000 rpm.

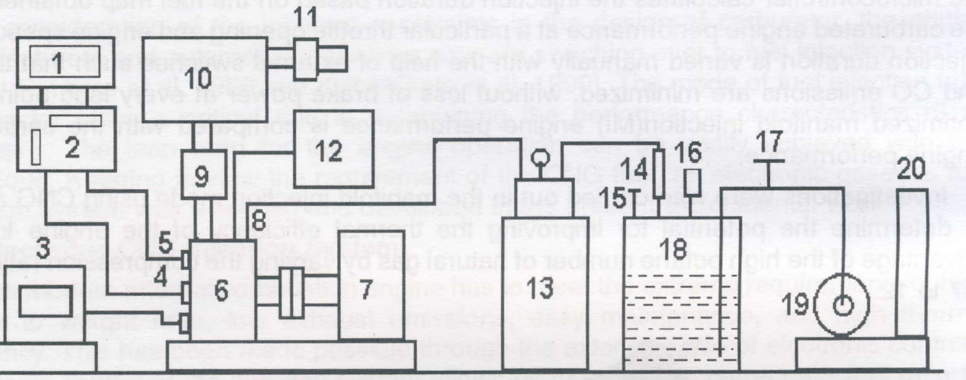

1. Computer	*2. Signal analyzer*	*3. Exhaust gas analyzer*
4. TDC pickup	*5. Pressure pickup*	*6. Engine*
7. Dynamometer	*8. Gas injector*	*9. Air filter*
10. Surge tank	*11. Air flow meter*	*12. Fuel injection system*
13. Stabilizing tank	*14. Gas rotameter .*	*15. Safety valve*
16. Pressure gauge	*17. Expansion valve*	*18. Flame trap*
19. CNG Cylinder	*20. Weighing machine*	

Figure. 2 Schematic diagram of experimental setup

4. RESULTS AND DISCUSSION

4.1 Brake Thermal Efficiency

Figures 3 to 6 shows the variation of brake thermal efficiency with brake mean effective pressure(BMEP) at different speeds for the manifold injection, and carbureted engine. The brake thermal efficiency in the manifold injection system is higher than the carbureted engine throughout the operating range at tested speeds.

Maximum brake thermal efficiency in manifold injection mode is 16.1% at 2500 rpm, 16.5% at 3000 rpm, 17.5% at 3500 rpm and 16.6% at 4000 rpm where as in carbureted engine at 2500 rpm is 14.1%, 14.4% at 3000 rpm, 15.2% at 3500 rpm and 14.8% at 4000 rpm.

The maximum increase in brake thermal efficiency in the manifold injection system compared to carbureted engine is 12.4% at 2500 rpm, 12.7% at 3000 rpm, 13.14% at 3500 rpm, and 12.6% at 4000 rpm. This is due to increase in air-fuel ratio and indicates that the engine can operate in leaner air-fuel ratios without loss of brake power. This is achieved because of the precise timing and metering of the fuel by the microcontroller fuel injection system.

Variation of brake thermal efficiency with equivalence ratio at 2500, 3000, 3500 and 4000 rpm are shown in Figures 7 to 10. Brake thermal efficiency increases with lean to rich mixture and further decreases as engine rich mixture continues. For the same equivalence ratio, the carbureted engine gives lesser brake thermal efficiency compared to the injected engine. This is due to incomplete combustion of the charge due to mixture limit inside the combustion chamber at a given compression ratio. Hence, the amount of fuel charge to give the mechanical power gets reduced and thus reduces the brake thermal efficiency.

4.2 Carbon Monoxide Emissions

Figures 11 to 14 show the variation of CO with equivalence ratio at 2500 rpm, 3000 rpm, 3500 rpm and 4000 rpm. Carbon monoxide, is the by product of incomplete combustion and totally dependent on the air fuel ratio. Owing to the gaseous nature of compressed natural gas, it easily mixes with air because of diffusivity at high pressure. CO emissions with lean mixture are reduced because of CO getting converted into CO2 with surplus amount of oxygen. In manifold injection mode, significant lower concentration of CO is observed over entire range of operation.

In manifold injection mode, lower concentration of CO is about 0.14% at 2500 rpm, 0.12% at 3000 rpm, 0.11% at 3500 rpm, and 0.10 % at 4000 rpm, where as in carbureted mode is 0.21% at 2500 rpm, 0.19% at 3000 rpm, 0.18 % at 3500 rpm, and 0.16% at 4000 rpm.

The maximum concentration of CO in manifold injection mode is 0.97%, 0.95%, 0.91%, and 0.85% at 2500, 3000, 3500 and at 4000 rpm respectively, where as in the carbureted mode is 1.12%, 1.1%, 1.06%, and 1.03% at 2500, 3000, 3500 and 4000 rpm respectively.

4.3 Hydrocarbon Emissions

Variation of HC emissions with equivalence ratio at different speeds is shown in Figs 15 to 18. The main source of hydrocarbons is due to the composition and patchy combustion occurring due to uneven mixture formation. Non-methane hydrocarbons are a strong function of the natural gas composition. As CNG is in gaseous state, the mixing of natural gas with the air is much better than that of gasoline with air. The concentration of hydrocarbons decreases with a decrease of equivalence ratio up to certain value and then increases. At much leaner air fuel ratios the HC concentration rapidly increases due to misfire.

The lower level of HC in the manifold injection mode at 2500 rpm is 1056 ppm, 945 ppm at 3000 rpm, 922 ppm at 3500 rpm and 835 ppm at 4000 rpm, where as in carbureted mode is 1325 ppm at 2500 rpm, 1090 ppm at 3000 rpm, 1100 ppm at 3500 rpm and 1040 ppm at 4000 rpm.

The maximum concentration of HC in the manifold injection mode is 2226 ppm at 2500 rpm, 2210 ppm at 3000 rpm, 2165 ppm at 3500 rpm and 2112 ppm at 4000 rpm, where as in the carbureted mode is 2512 ppm at 2500 rpm, 2418 ppm at 3000 rpm, 2310 ppm at 3500 rpm and 2283 ppm at 4000 rpm.

4.4 Coefficient of Variation of Peak Pressure and IMEP

Figures 19 to 22 show the variation of C.O.V. of peak pressure with BMEP at different speeds for manifold injection system and carbureted engine. The C.O.V. of peak pressure of the manifold injection system are lower than the carbureted engine at tested speeds and loads.

The maximum level of COV of peak pressure in the manifold injection mode is 8.8% at 2500 rpm, 6.9% at 3000 rpm, 6.6% at 3500 rpm, and 8.1% at 4000 rpm whereas in the carbureted engine is 13.3% at 2500 rpm, 14.1% at 3000 rpm, 11.2% at 3500 rpm and 13.4% at 4000 rpm.

The minimum level of COV of peak pressure in the manifold injection mode is 3.6% at 2500 rpm, 2.8% at 3000 rpm, 2.5% at 3500 rpm, and 3.7% at 4000 rpm, whereas in the carbureted mode is 6.2% at 2500 rpm, 7.8% at 3000 rpm, 6.8% at 3500 rpm, and 5.5% at 4000 rpm.

The maximum reduction in the C.O.V. of peak pressure in the manifold injection compared to carbureted engine is 41.9% at 2500 rpm, 64% at 3000 rpm, 63.2% at 3500 rpm, and 32% at 4000 rpm.

Figures 23 to 26 shows the variation of Coefficient of Variation of indicated mean effective pressure (C.O.V. of IMEP) with BMEP at different speeds for manifold injection system and carbureted engine. The C.O.V. of IMEP of the manifold injection system is lower than the carbureted engine at tested speeds and loads.

The maximum level of COV of IMEP in the manifold injection mode is 11% at 2500 rpm, 13.1% at 3000 rpm, 14.5% at 3500 rpm, and 14.1% at 4000 rpm, whereas in the carbureted engine is 25.1% at 2500 rpm, 21.2% at 3000 rpm, 23.4% at 3500 rpm, and 27.2% at 4000 rpm.

The minimum level of COV of IMEP in the manifold injection mode is 5% at 2500 rpm, 4.5%, at 3000 rpm, 6% at 3500 rpm, and 6.5% at 4000 rpm, where as in the carbureted mode is 8% at 2500 rpm, 7% at 3000 rpm, 7.5% at 3500 rpm, and 9% at 4000 rpm.

The maximum reduction in the C.O.V. of IMEP in the manifold injection compared to carbureted engine is 37.5% at 2500 rpm, 35.7% at 3000 rpm, 28.5 % at 3500 rpm, and 33.3% at 4000 rpm. The comparison between the COV in IMEP for carburetor type engine and manifold injection engine indicates that the fuel injected CNG engine is much more stable engine due to the better control of air fuel ratio.

4.5 Rate of Heat Release

The rate of heat release of the manifold injection system has increased by 16.2%, 14.3%, 17.7% and 22.72% at 2500, 3000, 3500 and 4000 rpm respectively compared to carbureted engine as shown in Figures 27 to 30. The increase in rate of heat release indicate that the combustion in the manifold injection is faster than the carbureted engine due to the combustion of the relatively lean air-fuel mixtures.

4.6 Results of Compression Ratio Investigation

A compression ratio investigation was carried out in the manifold injection (MI) mode using compressed natural gas as fuel to determine the potential of improving the thermal efficiency of an engine specially designed for natural gas to take advantage of the high octane number of natural gas[Ahmed E. Hassanen et al, 1998 and Fleming R.D, 1985]. The compression ratios investigated are 6.7:1, 8:1, 10:1, and 12:1.

Figures 31 to 34 show the variation of brake thermal efficiency with brake mean effective pressure for different compression ratio at 2500, 3000, 3500 and 4000 rpm respectively. Brake thermal efficiency increases with the increase in compression ratio (CR). The increase in brake thermal efficiency with compression ratio is due to higher in-cylinder temperatures and pressures. This increase also generates a higher level of turbulence in the cylinder and increases the combustion rate of the fuel/air charge. The wider flammability limits of natural gas-air mixtures and higher octane rating of fuel permit leaner than stoichiometric fuel-air ratio, which helps to improve engine thermal efficiency. The results clearly show that the compression ratio of 12:1 gave the highest brake thermal efficiency at different tested speeds.

The variation of brake thermal efficiency with equivalence ratio for different compression ratio at 2500, 3000, 3500 and 4000 rpm respectively are shown in Figures 35 to 38. It is clearly seen that the compression ratio of 12:1 gave the highest brake thermal efficiency at all the tested speeds. Brake thermal efficiency increases from lean to rich mixtures and starts decreasing at engine rich mixtures. The maximum brake thermal efficiency is in the range of equivalence ratio 0.85 to 1 at different speeds and the maximum efficiency was about 17.5% at 3500 rpm with a compression ratio of 12:1.

The variation of CO emission with equivalence ratio for different compression ratios is shown in Figures 39 to 42. It has been observed that, the CO emission reduces with an increase of compression ratio. This is due to more complete combustion taking place and the CO emission level gets reduced as the compression ratio increases.

Typical variations of the hydrocarbon emission with equivalence ratio at various compression ratios are shown in Figures 43 to 46. It has been observed that there is a reduction of hydrocarbons with an increase in the compression ratio. As CNG is in gaseous state, the mixture of natural gas with the air is better than that of gasoline with air. A condition leading to patchy combustion does not usually take place resulting in the reduction of HC emissions. Also, with an increase in the temperature of cylinder, the engine runs hotter thereby facilitating better and complete combustion. The cylinder walls and cylinder head are much hotter, and hence the tendency of flame quenching becomes less and production of lesser hydrocarbon emissions takes place [Bell.S.R, 1989; Das. A et al, 1997 and Evan, 1992]. The concentration of hydrocarbon emissions decreases with an increase of equivalence ratio up to a certain value and then it starts increasing. At much leaner air-fuel ratios the concentration of mixture in the combustion chamber varies giving rise to patchy combustion and thus increasing hydrocarbon emission. The mixture may also reduce the cylinder temperature causing flame quenching and increasing the hydrocarbon emissions. It has been observed from the results that the hydrocarbons are more at lean mixture and then decreases with equivalence ratio and once again increases with rich mixtures.

5. CONCLUSIONS

The performance of the manifold injection over the carbureted engine has the following improvements.

- Higher brake thermal efficiency
- Low HC and CO emissions
- Low C.O.V. of peak pressure and C.O.V. of IMEP
- Increase in the rate of heat release

These improvements are because of the fact that the manifold injection engine is able to operate at leaner equivalence ratio compared to the carbureted engine and precise timing and metering of fuel by the microcontroller fuel injection system.

6. REFERENCES

[1] Ahmed E. Hassanen and Keshav S. Varde., et al, "A study of the flame development and rapid burn duration in a lean burn fuel injected natural gas SI engine", SAE paper No. 981384, 1998.

[2] Bell.S.R. "Natural gas fuelling of a 2.5 litre spark ignited engine", 9th Miami International congress on energy and environment, 1989.

[3] Das. A and H.C. Watson., "Development of a natural gas spark ignition engine for optimum performance", Proceedings of international mechanical engineers, Vol. 211, part D, 1997.

[4] David Gimbres, Jacques Boree., et al., "Effect of air pulsed flow on the mixture preparation for the optimization of natural gas spark ignition engine," SAE paper No. 1999-01-2905, 1999.

[5] Douglass R and G.P. Blair., "Fuel injection of a two-stroke cycle spark ignition engine" SAE paper No. 820952, 1982.

[6] Edward F. Obert., "Low pressure electronic fuel injection system for two-stroke engines," SAE paper No. 780767, 1978.

[7] Evans.R.L., "Combustion design for a lean burn SI engine," SAE paper No. 921545, 1992.

[8] Fleming R.D. and G.B. O Neal., "Potential for improving the efficiency of spark ignition engine for natural gas fuel" SAE paper No. 852073, 1985.

[9] Giichi Yamagishi, Tadaniri Sto, and Hiroyoshi Iwasa., "A study of two stroke cycle fuel injection engines for exhaust gas purification" SAE paper No. 720195, 1972.

[10] Kichiro kato, et al., "Development of engine for natural gas engine," SAE paper No.1999-01-0574, 1999.

[11] Pipho.M J. and Kittelson. D.B., "Closed loop digital electronic control of diesel engine timing" SAE paper No.830579, 1983.

[12] Richard L.Bechtold .P.E., "Alternative fuels guide book" SAE, 1997.

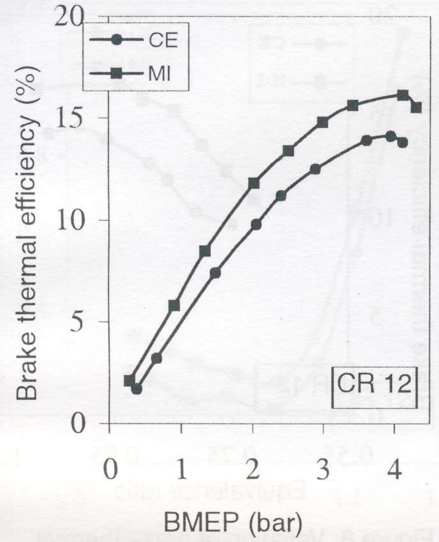

Figure 3: Variation of brake thermal efficiency with BMEP at 2500 rpm

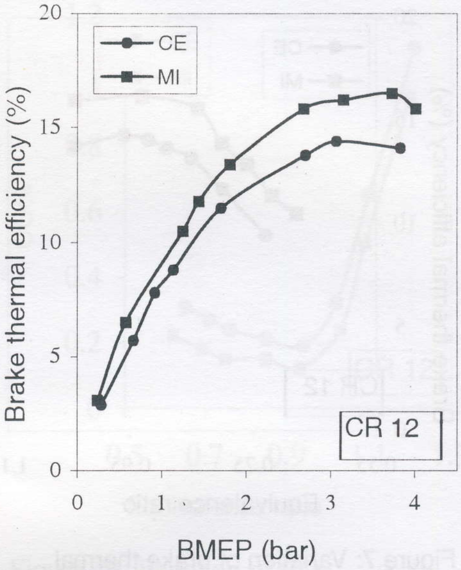

Figure 4: Variation of brake thermal efficiency with BMEP at 3000 rpm

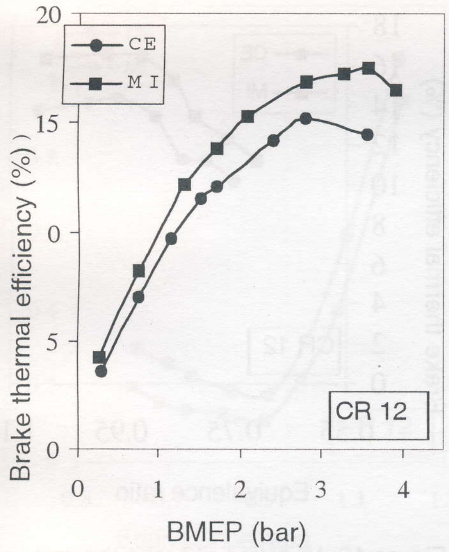

Figure 5: Variation of brake thermal efficiency with BMEP at 3500 rpm

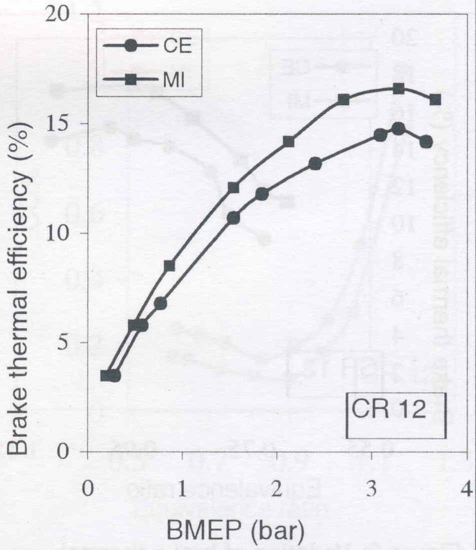

Figure 6: Variation of brake thermal efficiency with BMEP at 4000 rpm

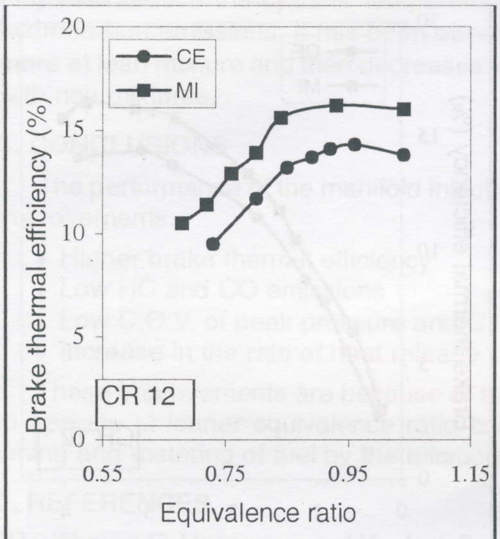

Figure 7: Variation of brake thermal efficiency with equivalence ratio at 2500 rpm

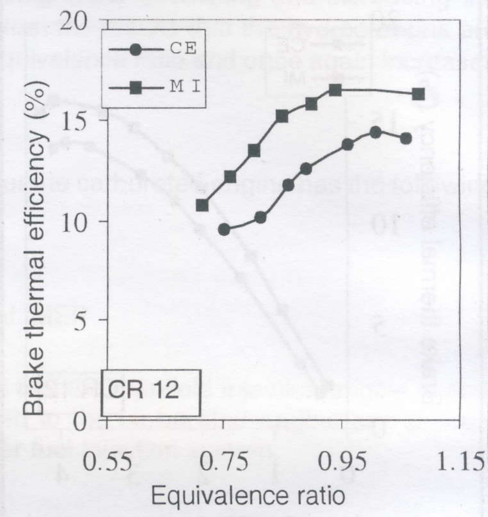

Figure 8: Variation of brake thermal efficiency with equivalence ratio at 3000 rpm

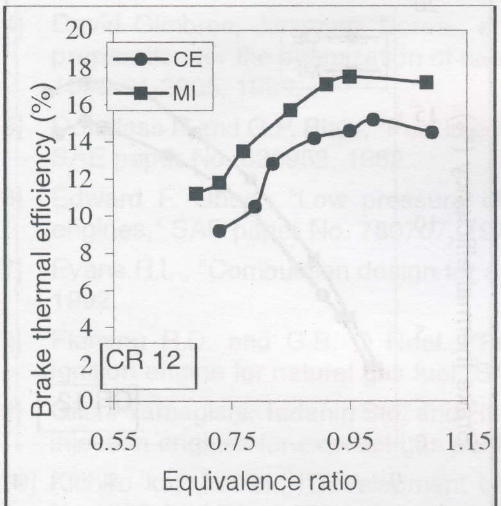

Figure 9: Variation of brake thermal efficiency with equivalence ratio at 3500 rpm

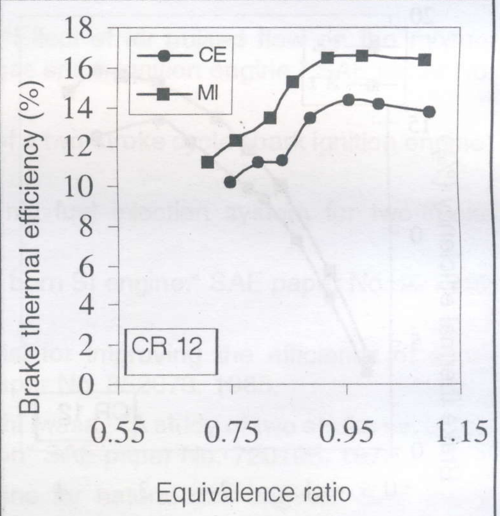

Figure 10: Variation of brake thermal efficiency with equivalence ratio at 4000 rpm

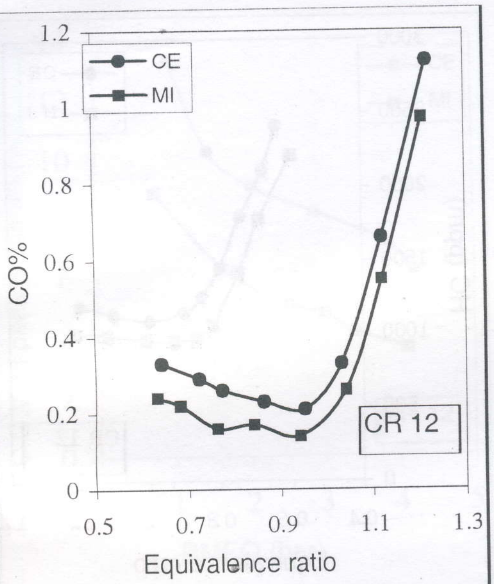

Figure 11: Variation of CO emissions with Equivalence ratio at 2500 rpm

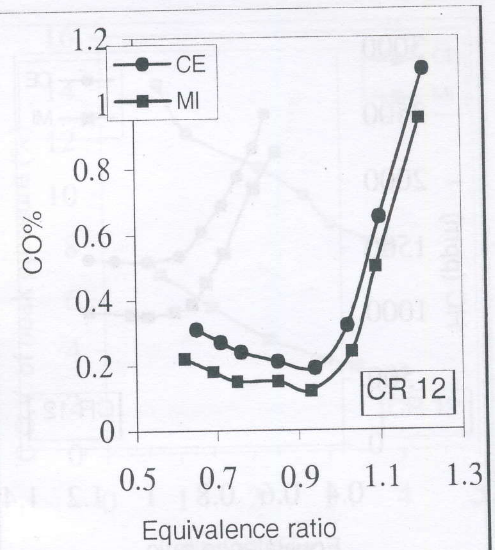

Figure 12: Variation of CO emissions with Equivalence ratio at 3000 rpm

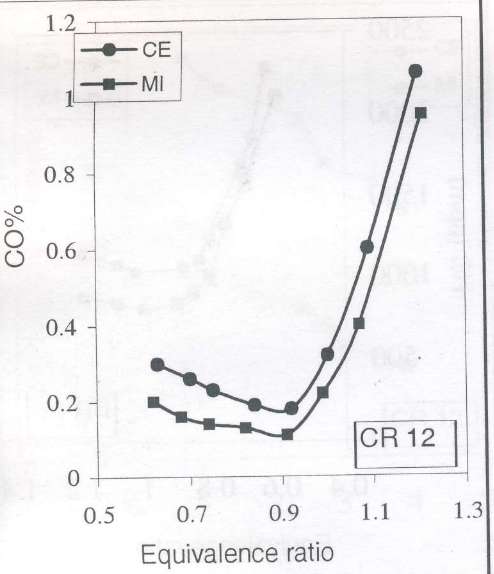

Figure 13: Variation of CO emissions with Equivalence ratio at 3500 rpm

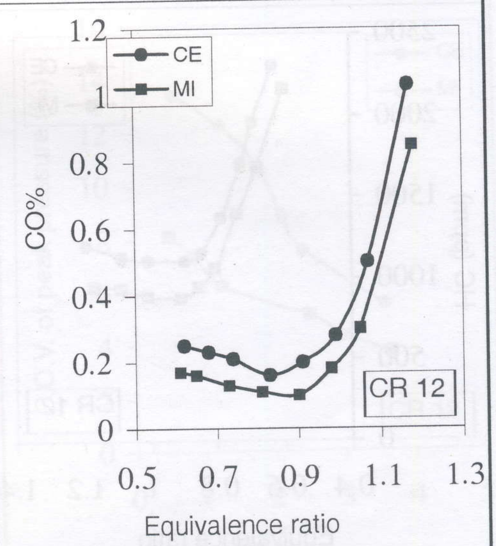

Figure 14: Variation of CO emissions with Equivalence ratio at 4000 rpm

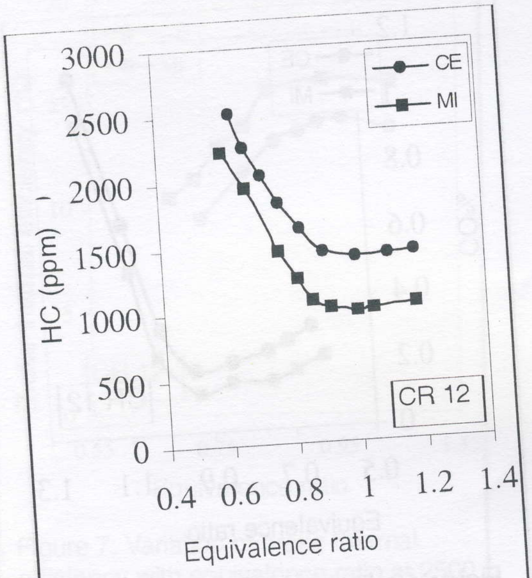

Figure 15: Variation of HC emissions with Equivalence ratio at 2500 rpm

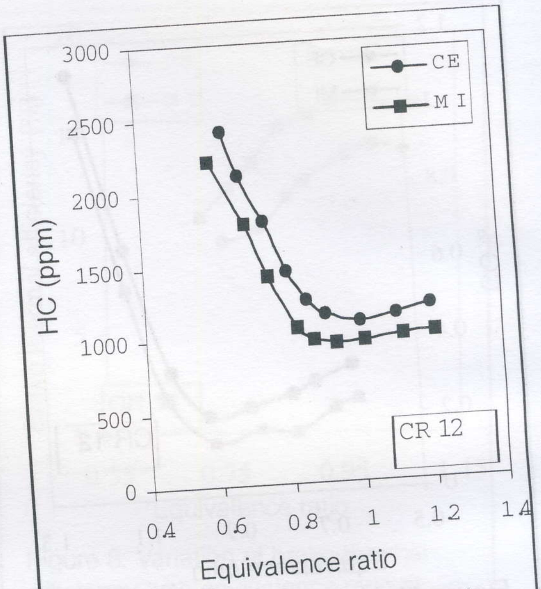

Figure 16: Variation of HC emissions with Equivalence ratio at 3000 rpm

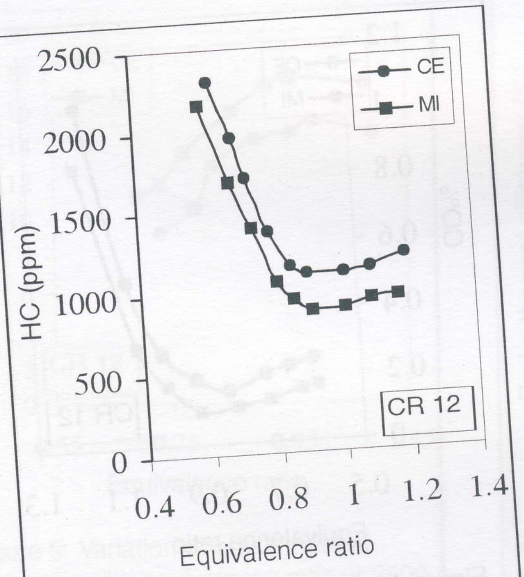

Figure 17: Variation of HC emissions with Equivalence ratio at 3500 rpm

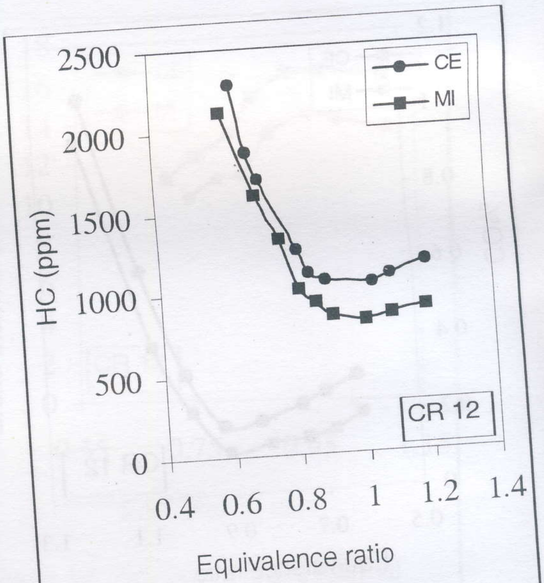

Figure 18: Variation of HC emissions with Equivalence ratio at 4000 rpm

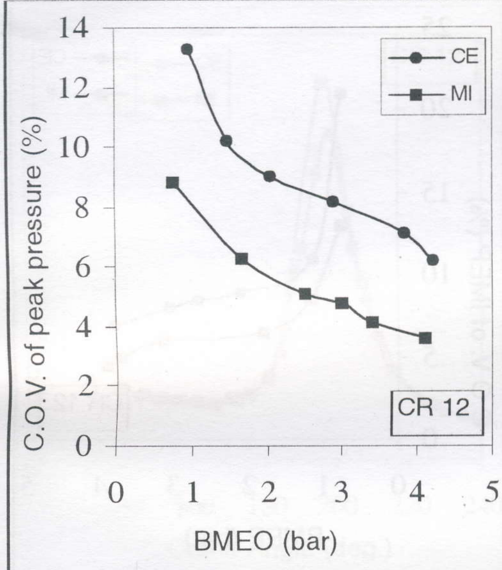

Figure 19: Variation of C.O.V of peak pressure with BMEP at 2500 rpm

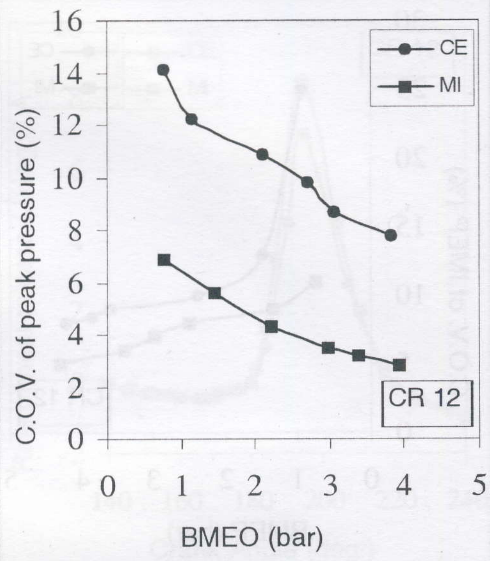

Figure 20: Variation of C.O.V of peak pressure with BMEP at 3000 rpm

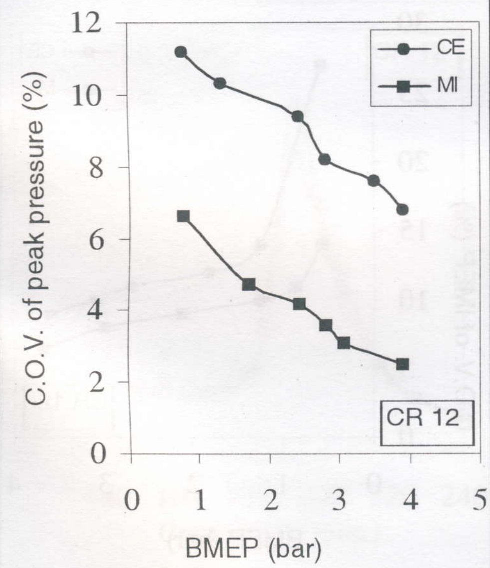

Figure 21: Variation of C.O.V of peak pressure with BMEP at 3500 rpm

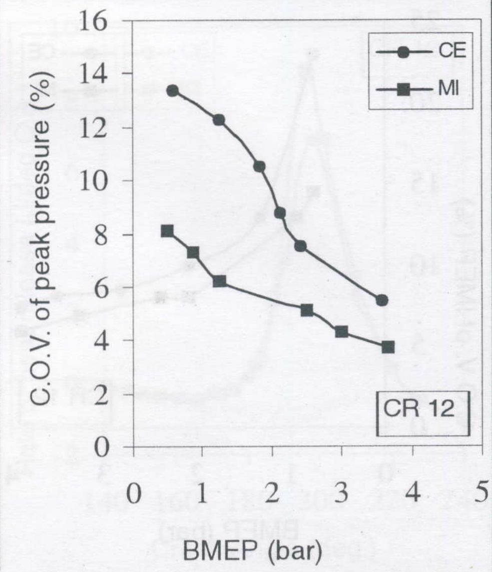

Figure 22: Variation of C.O.V of peak pressure with BMEP at 4000 rpm

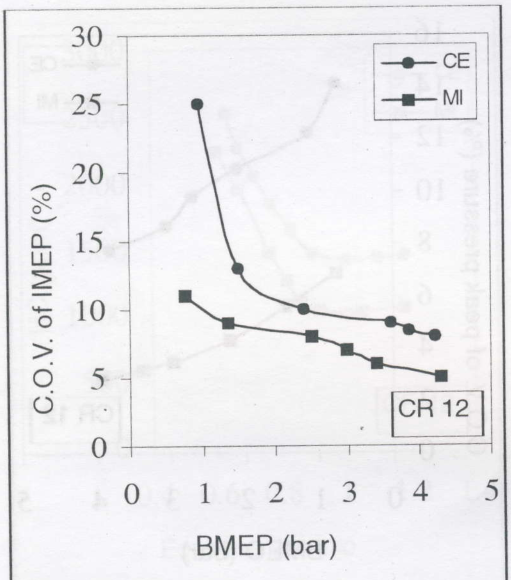

Figure 23: Variation of C.O.V of IMEP with BMEP at 2500 rpm

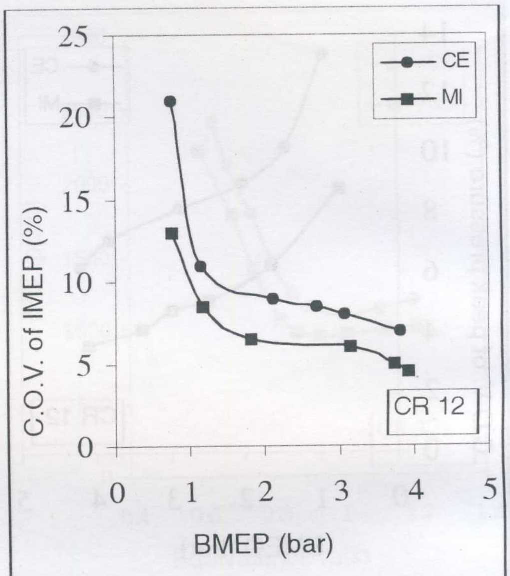

Figure 24: Variation of C.O.V of IMEP with BMEP at 3000 rpm

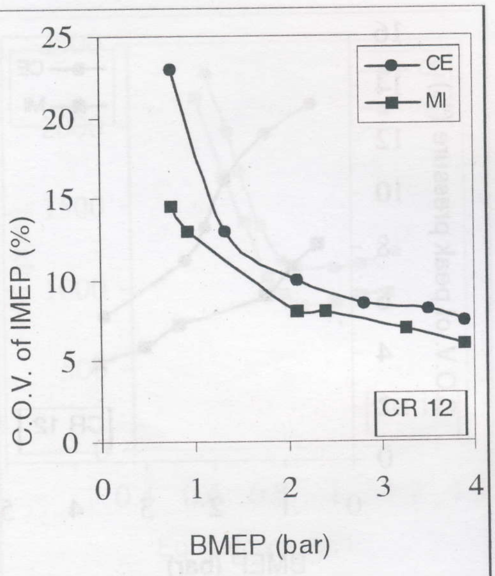

Figure 25: Variation of C.O.V of IMEP with BMEP at 3500 rpm

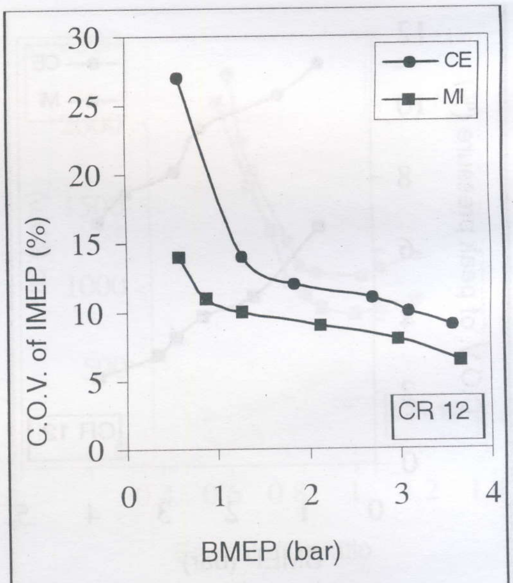

Figure 26: Variation of C.O.V of IMEP with BMEP at 4000 rpm

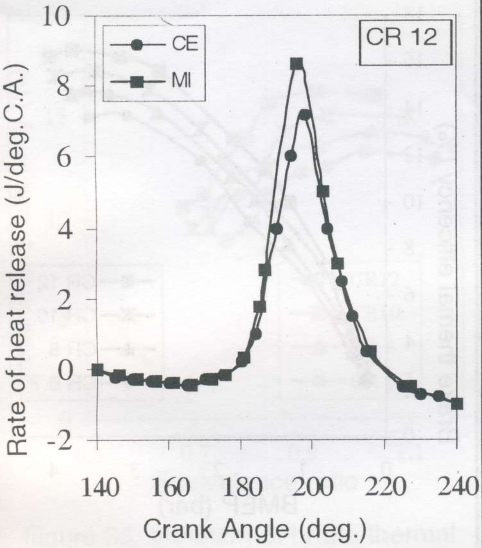

Figure 27: Variation of rate of heat release at 2500 rpm

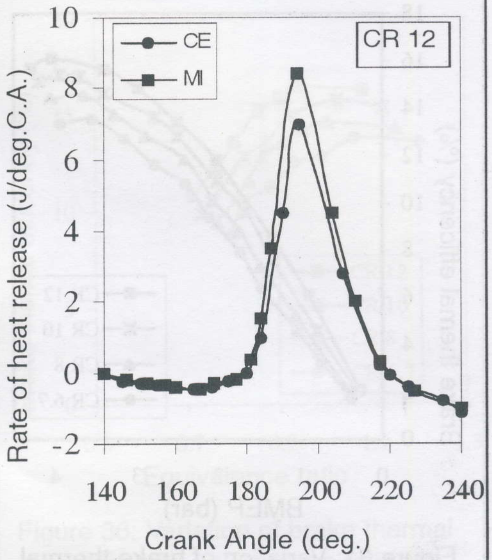

Figure 28: Variation of rate of heat release at 3000 rpm

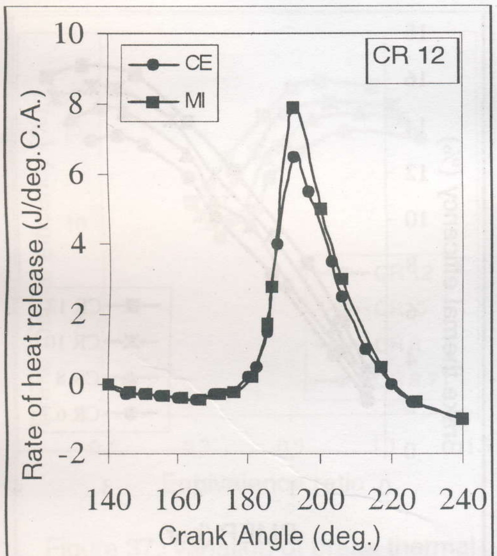

Figure 29: Variation of rate of heat release at 3500 rpm

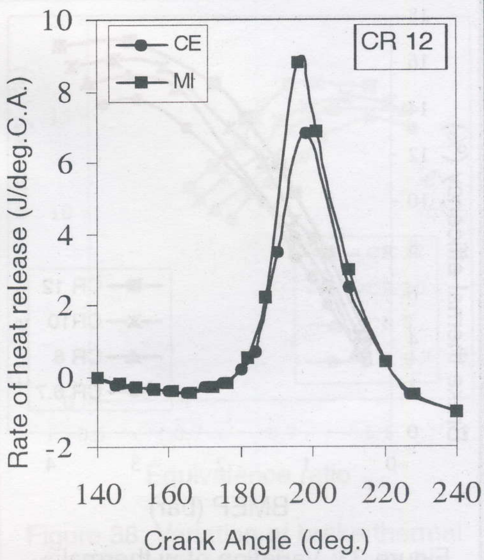

Figure 30: Variation of rate of heat release at 4000 rpm

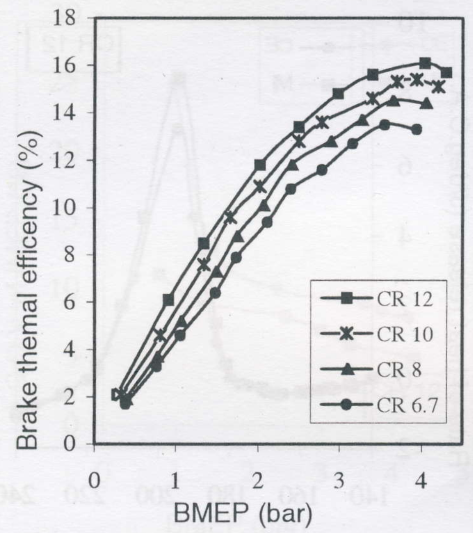

Figure 31: Variation of brake thermal efficiency with BMEP for different compression ratio at 2500 rpm

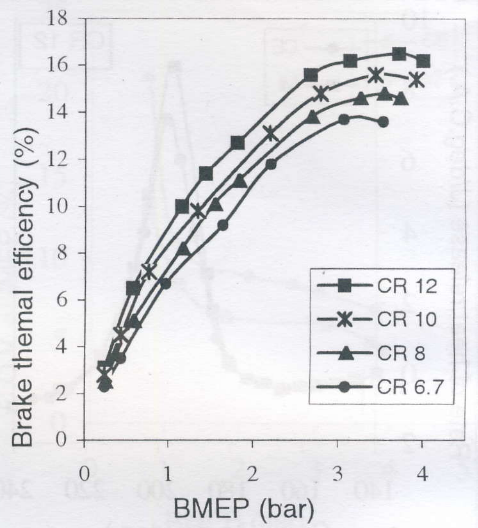

Figure 32: Variation of brake thermal efficiency with BMEP for different compression ratio at 3000 rpm

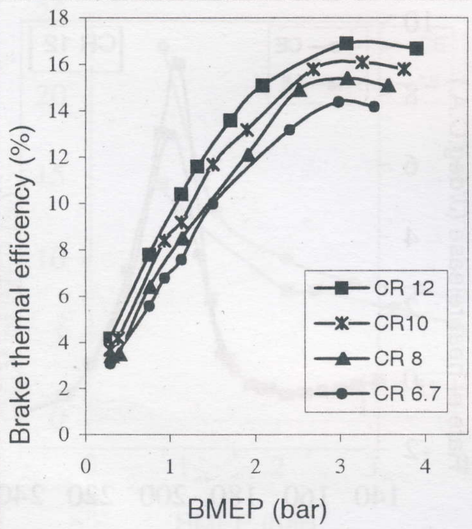

Figure 33: Variation of w thermal efficiency with BMEP for different compression ratio at 3500 rpm

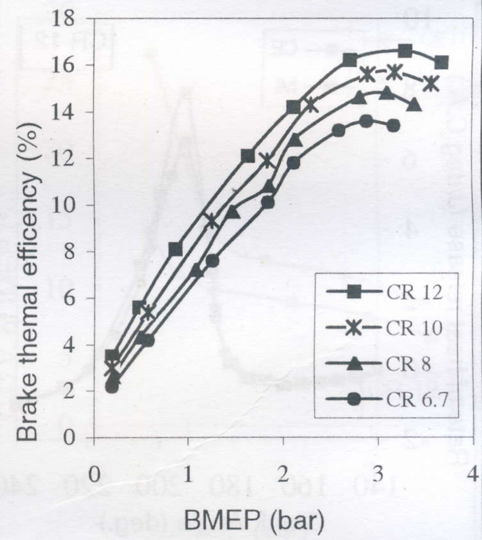

Figure 34: Variation of brake thermal efficiency with BMEP for different compression ratio at 4000 rpm

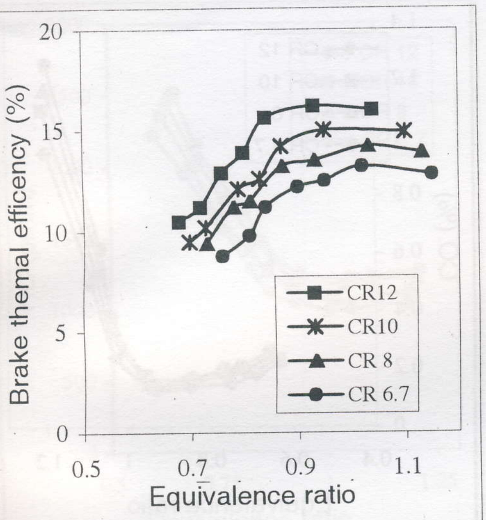

Figure 35: Variation of brake thermal efficiency with equivalence ratio for different compression ratio at 2500 rpm

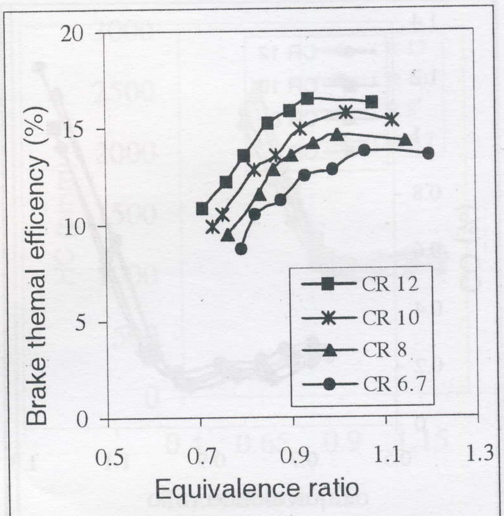

Figure 36: Variation of brake thermal efficiency with equivalence ratio for different compression ratio at 3000 rpm

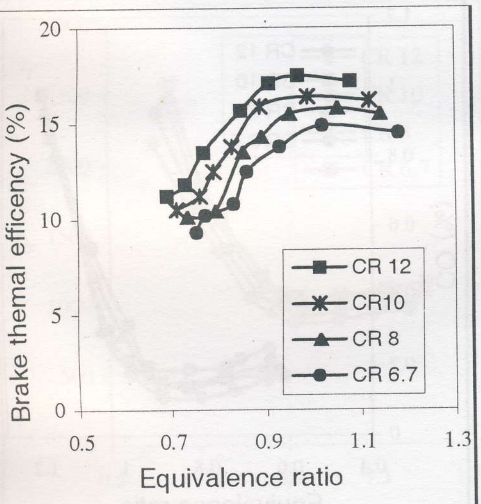

Figure 37: Variation of brake thermal efficiency with equivalence ratio for different compression ratio at 3500 rpm

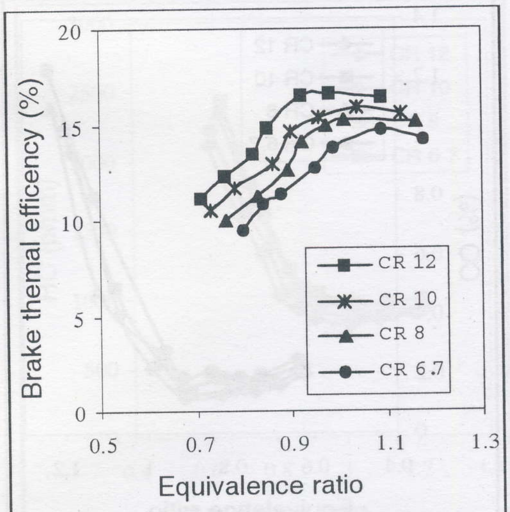

Figure 38: Variation of brake thermal efficiency with equivalence ratio for different compression ratio at 4000 rpm

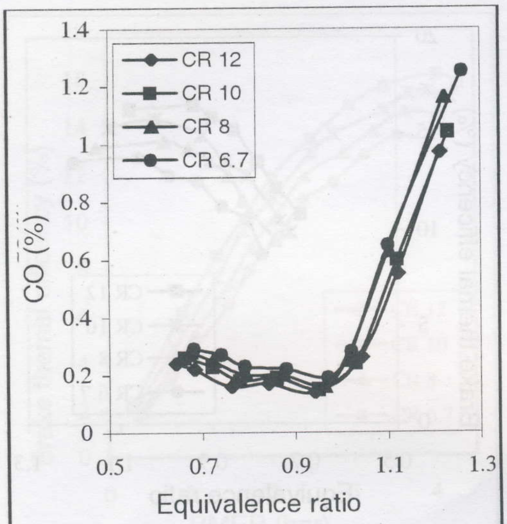

Figure 39: Variation of CO emissions with equivalence ratio for different compression ratio at 2500 rpm

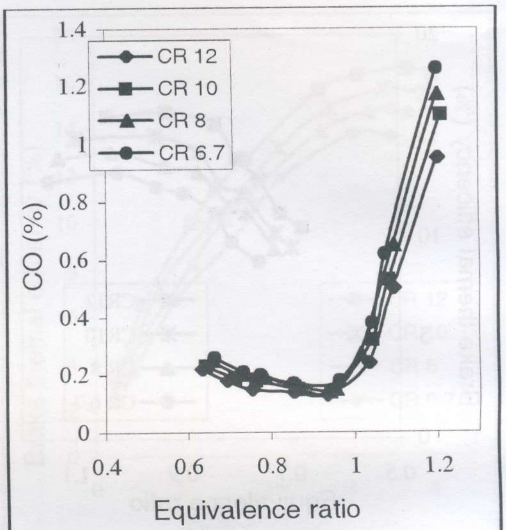

Figure 40: Variation of CO emissions with equivalence ratio for different compression ratio at 3000 rpm

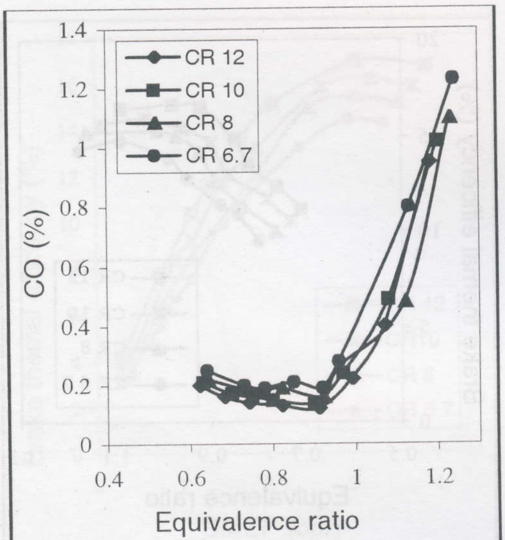

Figure 41: Variation of CO emissions with equivalence ratio for different compression ratio at 3500 rpm

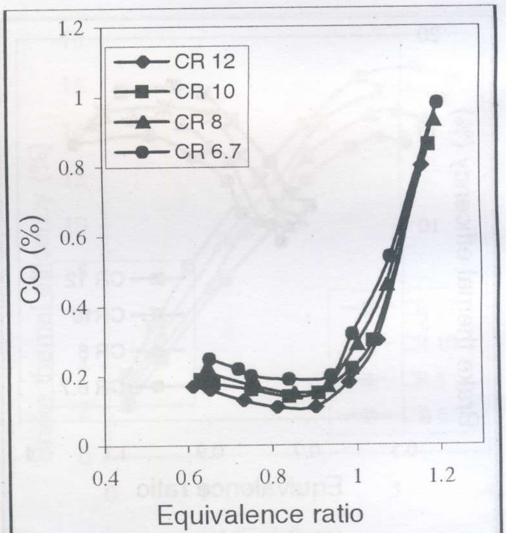

Figure 42: Variation of CO emissions with equivalence ratio for different compression ratio at 4000 rpm

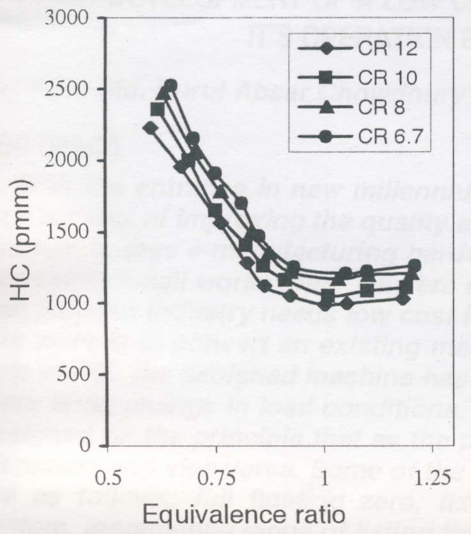

Figure 43: Variation of HC emissions with equivalence ratio for different compression ratio at 2500 rpm

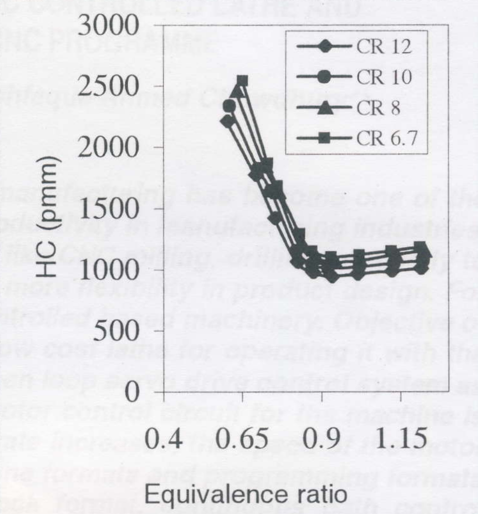

Figure 44: Variation of HC emissions with equivalence ratio for different compression ratio at 3000 rpm

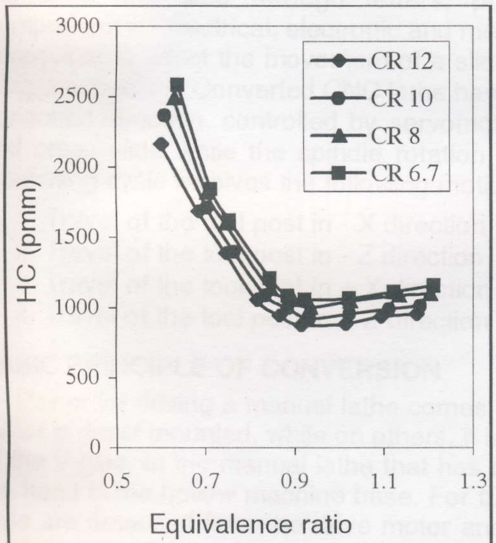

Figure 45: Variation of HC emissions with equivalence ratio for different compression ratio at 3500 rpm

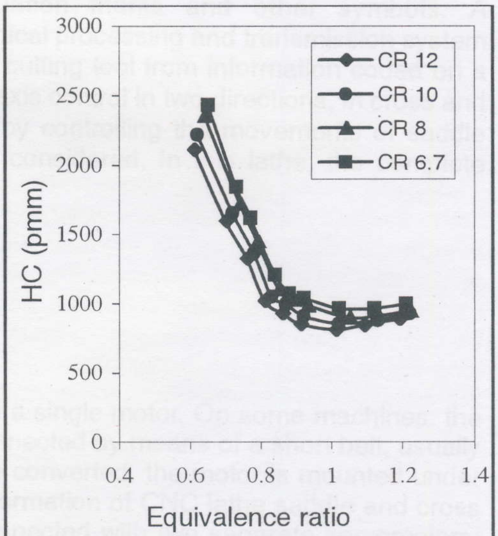

Figure 46: Variation of HC emissions with equivalence ratio for different compression ratio at 4000 rpm